

Quaternion colour representations and derived total orderings for morphological operators

Jesús Angulo; Centre de Morphologie Mathématique - Ecole des Mines de Paris; 35, rue Saint-Honoré, 77305 Fontainebleau cedex - France

Abstract

The definition of morphological operators for colour images needs a total ordering between the colour points. A colour can be represented according to different algebraic structures, in particular in this paper we focus on real quaternions. The paper presents two main contributions. On the one hand, we have studied different alternatives to introduce the scalar part to obtain full colour quaternions. On the other hand, several total lexicographic orderings for quaternions according to their different decompositions have been defined. These quaternionic orderings have been characterised in order to identify the most useful to define morphological operators for colour images. The theoretical results are illustrated with examples of processed images.

Introduction

Let $\mathbf{c}_i = (r_i, g_i, b_i)$ be the triplet of the red, green and blue intensities for the pixel i of a digital colour image. The definition of morphological operators for colour images needs a total ordering \leq_{Ω} between the colour points, i.e., for any pair of unequal points \mathbf{c}_i and \mathbf{c}_j it should be possible to verify if $\mathbf{c}_i \leq_{\Omega} \mathbf{c}_j$ or if $\mathbf{c}_i \geq_{\Omega} \mathbf{c}_j$, in order to be able to compute the erosion (as the infimum) and the dilation (as the supremum) of any subset of RGB colour set \mathcal{T}^{rgb} ; or in other words, $(\mathcal{T}^{rgb}, \leq_{\Omega})$ must be a complete lattice. In the literature, many techniques have been proposed on the extension of mathematical morphology to colour images. An exhaustive state-of-the-art has been reported in recent papers [3] [4].

The point \mathbf{c}_i can be represented according to different algebraic structures, in particular in this paper we focus on real quaternions [10]. We explore here the way to build colour quaternions from a RGB triplet and the different alternatives to define total orderings based on the specific properties of two quaternion representations (polar form and parallel/perpendicular decomposition), characterising and identifying the most useful to define nonlinear morphological operators. The theoretical results are illustrated with examples of processed images.

Quaternion-based colour operations, such as colour Fourier transform, colour convolution and linear filters, have been studied mainly by [7, 12, 8] and by [6, 5].

From RGB colours to colour quaternions: The choice of the scalar part

Quaternions and product of quaternions

A quaternion $\mathbf{q} \in \mathbb{H}$ may be represented in hypercomplex form as

$$\mathbf{q} = a + bi + cj + dk, \quad (1)$$

where a, b, c and d are real. A quaternion has a *real part or scalar part*, $S(\mathbf{q}) = a$, and an *imaginary part or vector part*, $V(\mathbf{q}) = bi + cj + dk$, such that the whole quaternion may be represented by the sum of its scalar and vector parts as $\mathbf{q} = S(\mathbf{q}) + V(\mathbf{q})$. A quaternion with a zero real/scalar part is called a *pure quaternion*.

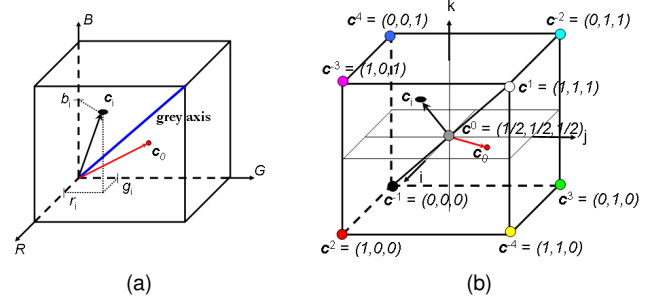


Figure 1. RGB colour spaces: (a) Unitary cube C , (b) Centered cube, representing the nine dominant colours.

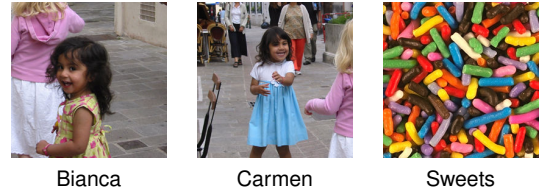


Figure 2. Original colour images, $f(x)$, used in the paper.

The addition of two quaternions, $\mathbf{q}, \mathbf{q}' \in \mathbb{H}$, is defined as follows $\mathbf{q} + \mathbf{q}' = (a + a') + (b + b')i + (c + c')j + (d + d')k$. The addition is commutative and associative.

The quaternion result of the *product of two quaternions* is defined as

$$\mathbf{q}'' = \mathbf{q}\mathbf{q}' = (aa' - bb' - cc' - dd') + (ab' + ba' + cd' - dc')i + (ac' + ca' + db' - bd')j + (ad' + d'a + bc' - cb')k \quad (2)$$

which can be also written in terms of dot and cross product of vectors: $\mathbf{q}'' = \mathbf{q}\mathbf{q}' = S(\mathbf{q}'') + V(\mathbf{q}'')$, with $S(\mathbf{q}'') = S(\mathbf{q})S(\mathbf{q}') - V(\mathbf{q}) \cdot V(\mathbf{q}')$, and $V(\mathbf{q}'') = S(\mathbf{q})V(\mathbf{q}') + S(\mathbf{q}')V(\mathbf{q}) + V(\mathbf{q}) \times V(\mathbf{q}')$, where \cdot and \times represent the dot product vector and the cross product vector respectively. The multiplication of quaternions is not commutative, i.e., $\mathbf{q}\mathbf{q}' \neq \mathbf{q}'\mathbf{q}$; but it is associative.

Colour quaternions

According to the previous works on the representation of colour by quaternions, we consider the gray-centered RGB colour-space [7]. In this space, the unit RGB cube is translated so that the coordinate origin $\hat{O}(0,0,0)$ represents mid-gray (middle point of the gray axis or half-way between black and white), see Fig 1(b). Then, a colour can be represented by a pure quaternion: $\mathbf{c}_i = (r, g, b) \Rightarrow \mathbf{q}_i = i\hat{r} + j\hat{g} + k\hat{b}$, where $\hat{\mathbf{c}} = (\hat{r}, \hat{g}, \hat{b}) = (r - 1/2, g - 1/2, b - 1/2)$.

It should be remarked that in this centered RGB color space the black colour quaternion and the white colour quaternion play

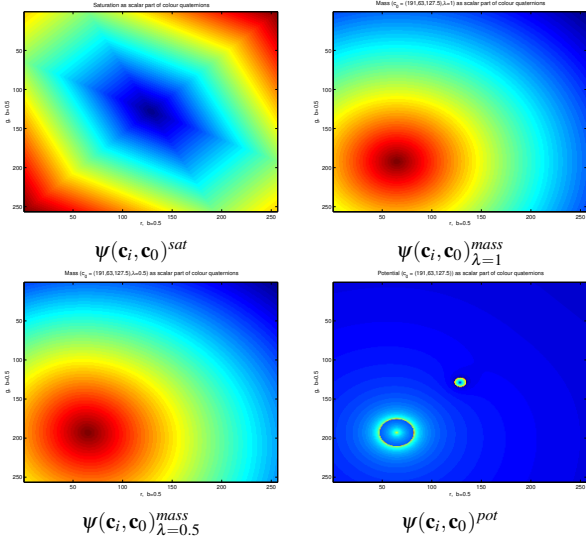


Figure 3. Variation of different scalar parts $\psi(\mathbf{c}_i, \mathbf{c}_0)$ in the plane (r, g) , $b = 0.5$, of the RGB cube, where the reference colour is $\mathbf{c}_0 = (0.75, 0.25, 0.50)$.

a symmetrical role in terms of distance to the center and the same is true for any pair of complementary colours.

In order to better exploit the power of quaternion algebra, we propose here to introduce a scalar part for each colour quaternion, i.e.,

$$\mathbf{c}_i = (r, g, b) \Rightarrow \mathbf{q}_i = \psi(\mathbf{c}_i, \mathbf{c}_0) + i\hat{r} + j\hat{g} + k\hat{b}. \quad (3)$$

The scalar component, $\psi(\mathbf{c}_i, \mathbf{c}_0)$, is a real value obtained from the colour point i and a colour of reference $\mathbf{c}_0 = (r_0, g_0, b_0)$. The reference \mathbf{c}_0 can be for instance the white point $(1, 1, 1)$, but also any other colour which should impose a particular effect of the associated operator.

We have considered three possible definitions for the scalar part. In order to understand the different alternatives we give in Fig. 3 the values in the plane (r, g) , $b = 0.5$, for several examples.

1) Saturation:

$$\psi(\mathbf{c}_i, \mathbf{c}_0)^{sat} = s_i = \begin{cases} \frac{3}{2}(max_i - m_i) & \text{if } m_i \geq med_i \\ \frac{3}{2}(m_i - min_i) & \text{if } m_i \leq med_i, \end{cases} \quad (4)$$

where $m_i = (r_i + g_i + b_i)/3$, $max_i = \max(r_i, g_i, b_i)$, $min_i = \min(r_i, g_i, b_i)$ and med_i is the median value of the triplet (r_i, g_i, b_i) . In fact, s_i is the saturation of the luminance/saturation/hue representation in norm L_1 [2], obtained as the modulus of the projected colour vector on the chromatic plane (i.e., the plane orthogonal to the grey axis in the origin), see the example in Fig. 3. Obviously, the value of saturation for \mathbf{c}_i does not depend on the reference colour \mathbf{c}_0 .

The saturation is the chromatic variety of a colour (i.e., the degree of dilution, inverse to the quantity of ‘‘white’’ of the colour) and it can not be obtained as a simple linear combination of RGB values in contrast to the luminance (which is typically the norm of the vector (r_i, g_i, b_i)). This is the rationale behind the appropriateness of $\psi(\mathbf{c}_i, \mathbf{c}_0)^{sat}$ as scalar value for the colour quaternion.

2) Mass with respect to \mathbf{c}_0 :

$$\psi(\mathbf{c}_i, \mathbf{c}_0)_\lambda^{mass} = \exp\left(-w_E \|\mathbf{c}_i - \mathbf{c}_0\| - w_\angle \arccos\left(\frac{\mathbf{c}_i \cdot \mathbf{c}_0}{\|\mathbf{c}_i\| \|\mathbf{c}_0\|}\right)\right),$$

(5)

where $w_E = (1/\sqrt{2})\lambda$ and $w_\angle = (2\pi)^{-1}(1 - \lambda)$. It is a decreasing function of a linear barycentric combination of two colour distances between \mathbf{c}_i and the reference colour \mathbf{c}_0 . The value of $0 \leq \lambda \leq 1$ allows to weigh up the influence of the Euclidean distance (i.e., RGB uniform distance) between both colours with respect to the angle distance (i.e., chromatic distance equivalent to a hue distance). Fig. 3 provides two examples for $\lambda = 1$ and $\lambda = 0.5$; this last well-balanced choice is adopted in subsequent examples in order to integrate both kinds of colour distances.

Consequently, the value of the scalar component $\psi(\mathbf{c}_i, \mathbf{c}_0)_\lambda^{mass}$ is maximal for $\mathbf{c}_i = \mathbf{c}_0$ and decreases when the colour \mathbf{c}_i gets away from the reference \mathbf{c}_0 . In any case, the values are always positive and can be normalised in order to have the same dynamics as the colour quaternion complex components.

3) Potential with respect to \mathbf{c}_0 and the nine significant colour points in the RGB unit cube:

$$\psi(\mathbf{c}_i, \mathbf{c}_0)^{pot} = \phi_E^+ + \phi_E^- = \frac{\kappa^+}{4\pi\epsilon_0 \|\mathbf{c}_i - \mathbf{c}_0\|} + \sum_{n=-4, n \neq i}^4 \frac{\kappa^-}{4\pi\epsilon_0 \|\mathbf{c}_i - \mathbf{c}^n\|}, \quad (6)$$

where the positive potential ϕ_E^+ represents the influence of a positive charge placed at the position of the reference colour \mathbf{c}_0 and the negative term ϕ_E^- corresponds to the potential associated to nine negative charges in the significant colours of the RGB cube: i) the three main achromatic points which are the extremes of the main diagonal of the cube (black $\mathbf{c}^{-1} = (0, 0, 0)$ and white $\mathbf{c}^1 = (1, 1, 1)$), grey axis or luminance axis, and the mid-gray or center of the diagonal ($\mathbf{c}^0 = (1/2, 1/2, 1/2)$), which is also the center of the cube; ii) the three chromatic primaries, i.e., red $\mathbf{c}^2 = (1, 0, 0)$, green $\mathbf{c}^3 = (0, 1, 0)$ and blue $\mathbf{c}^4 = (0, 0, 1)$; and iii) the three chromatic complementary primaries, i.e., cyan $\mathbf{c}^{-2} = (0, 1, 1)$, magenta $\mathbf{c}^{-3} = (1, 0, 1)$ and yellow $\mathbf{c}^{-4} = (1, 1, 0)$. Note that for each primary point j ($2 \leq j \leq 4$) the corresponding complementary, or anti-primary $-j$, is the opposite point in the cube.

This function $\psi(\mathbf{c}_i, \mathbf{c}_0)^{pot}$ balances the influence of the reference point with respect to the significant points of the RGB unit cube C , see Fig. 1.

Typically, to equilibrate both kinds of charges, it is taken $\kappa^+ = 9Q$ and $\kappa^- = -Q$, and in order to make easier the computation we fix $Q = \mu/(4\pi\epsilon_0)$. The value of constant μ allows to control the dynamics of this scalar part with respect to the other quaternion components.

Quaternion colour representations and associated total orderings

Two interesting quaternion representations

1) Quaternion colour polar form: Any quaternion may be represented in polar form as $\mathbf{q} = \rho e^{\xi\theta}$, with $\rho = \sqrt{a^2 + b^2 + c^2 + d^2}$, $\xi = \frac{bi+cj+dk}{\sqrt{b^2+c^2+d^2}}$ and $\theta = \arctan\left(\frac{\sqrt{b^2+c^2+d^2}}{a}\right)$.

In this polar formulation, $\rho = |\mathbf{q}|$ is the modulus of \mathbf{q} ; ξ is the pure unitary quaternion associated to \mathbf{q} (by the normalisation, the quaternion representation of a colour discards distance information, but retains orientation information relative to mid-gray, which correspond in fact to the chromatic or hue-related information.), sometimes called *eigenaxis*; and θ is the angle, sometimes called *eigenangle*, between the real part and the 3D imaginary part.

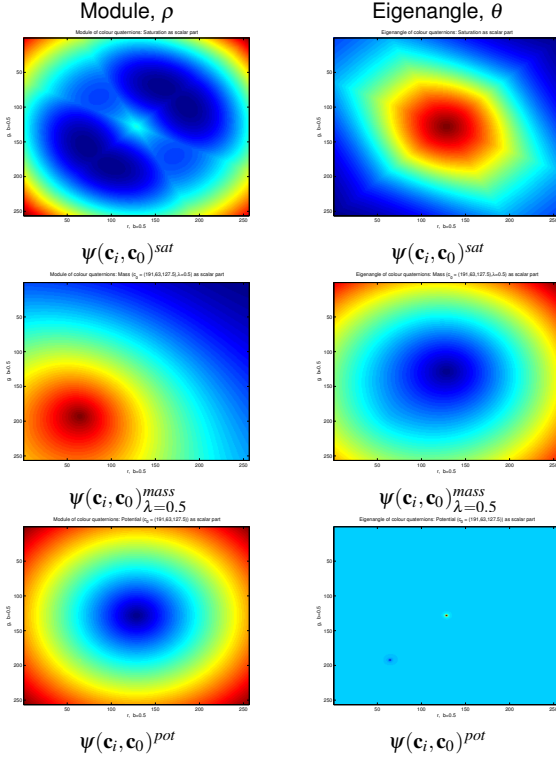


Figure 4. Variation of modulus ρ_i and eigenangle θ_i of colour quaternions \mathbf{q}_i according to the different scalar parts in the plane (r, g) , $b = 0.5$, of the RGB cube, where the reference colour is $\mathbf{c}_0 = (0.75, 0.25, 0.50)$.

The eigenaxis of a colour quaternion, ξ_i , is independent of its scalar part. The imaginary term $b^2 + c^2 + d^2 = (r_i - 1/2)^2 + (g_i - 1/2)^2 + (b_i - 1/2)^2$ is the norm of the colour vector in the centered cube and can be considered as a perceived energy of the colour (i.e., relative energy with respect to the mid-gray), being maximal for the eight significant colours associated to the cube corners. Note that the black and white have the same value as the six chromatic colours. The modulus ρ_i is an additive combination of the imaginary part and the scalar part. In Fig. 4 are shown the values of ρ_i according to the chosen scalar part. In the same figure are also given the corresponding values for the eigenangle θ_i . The function arctan (four-quadrant inverse tangent) is defined in the interval $[-\pi/2, \pi/2]$. If $\psi(\mathbf{c}_i, \mathbf{c}_0)$ is positive (it is always the case for saturation and mass with respect to \mathbf{c}_0), the value of θ_i is ≥ 0 and it increases when the ratio $\sqrt{(r_i - 1/2)^2 + (g_i - 1/2)^2 + (b_i - 1/2)^2} / \psi(\mathbf{c}_i, \mathbf{c}_0)$ increases. The value of $\psi(\mathbf{c}_i, \mathbf{c}_0)$ can be negative for the potential scalar part and in this case θ_i is negative and decreasing with respect to the absolute value of the ratio. Consequently, even if θ_i gives an angular value, we can consider the eigenangle as a totally ordered function.

2) Quaternion parallel/perpendicular decomposition [7]: Using the product of quaternions, it is possible to describe vector decompositions. A full quaternion \mathbf{q} may be decomposed about a pure unit quaternion \mathbf{p}^u :

$$\mathbf{q} = \mathbf{q}_\perp + \mathbf{q}_\parallel,$$

the *parallel part* of \mathbf{q} according to \mathbf{p}^u , also called the *projection part*, is given by $\mathbf{q}_\parallel = S(\mathbf{q}) + V_\parallel(\mathbf{q})$, and the *perpendicular part*, also named the *rejection part*, is obtained as $\mathbf{q}_\perp = V_\perp(\mathbf{q})$ where

$$V_\parallel(\mathbf{q}) = \frac{1}{2}(V(\mathbf{q}) - \mathbf{p}^u V(\mathbf{q}) \mathbf{p}^u)$$

and

$$V_\perp(\mathbf{q}) = \frac{1}{2}(V(\mathbf{q}) + \mathbf{p}^u V(\mathbf{q}) \mathbf{p}^u).$$

In Fig. 5 is depicted an example illustrating this \parallel/\perp decomposition. We should remind that the product of quaternions is computed according to the Rel.(2).

In the case of colour quaternions, \mathbf{p}^u corresponds to the pure unit quaternion associated to the reference colour \mathbf{c}_0 , which is denoted \mathbf{q}_0^u . Fig. 6 gives the variation of the module of the parallel quaternion, $|\mathbf{q}_\parallel|$, and the module of the perpendicular quaternion, $|\mathbf{q}_\perp|$, according to two examples of reference quaternion \mathbf{q}_0^u . It should be remarked that the rejection part is a pure quaternion and that the value is independent of the scalar part of \mathbf{q} , but, of course, it depends on the reference colour used for the decomposition.

Total orderings for colour quaternions

Using these representations, two main families of lexicographical-based partial ordering between colour quaternions can be defined.

1) Polar-based orderings: To order according to a priority in the choice of the polar parameters of the quaternion. The ordering, $\leq_{\Omega_1^{\mathbf{q}_0^u}}$, imposes the priority to the modulus, i.e.,

$$\mathbf{q}_i \leq_{\Omega_1^{\mathbf{q}_0^u}} \mathbf{q}_j \Leftrightarrow \begin{cases} \rho_i < \rho_j \text{ or} \\ \rho_i = \rho_j \text{ and } \theta_i < \theta_j \text{ or} \\ \rho_i = \rho_j \text{ and } \theta_i = \theta_j \text{ and } \|\xi_i - \xi_0\| \geq \|\xi_j - \xi_0\| \end{cases}$$

In this ordering, for two colour quaternions having the same module is bigger the quaternion with bigger eigenangle or if equals, with lower chromatic distance to the reference colour.

Two other orderings can be defined, giving respectively the priority to the value of the eigenangle or to the distance between the eigenaxis and $\mathbf{q}_0^u = \xi_0$, i.e.,

$$\mathbf{q}_i \leq_{\Omega_2^{\mathbf{q}_0^u}} \mathbf{q}_j \Leftrightarrow \begin{cases} \theta_i < \theta_j \text{ or} \\ \theta_i = \theta_j \text{ and } \rho_i < \rho_j \text{ or} \\ \theta_i = \theta_j \text{ and } \rho_i = \rho_j \text{ and } \|\xi_i - \xi_0\| \geq \|\xi_j - \xi_0\| \end{cases}$$

and

$$\mathbf{q}_i \leq_{\Omega_3^{\mathbf{q}_0^u}} \mathbf{q}_j \Leftrightarrow \begin{cases} \|\xi_i - \xi_0\| > \|\xi_j - \xi_0\| \text{ or} \\ \|\xi_i - \xi_0\| = \|\xi_j - \xi_0\| \text{ and } \rho_i < \rho_j \text{ or} \\ \|\xi_i - \xi_0\| = \|\xi_j - \xi_0\| \text{ and } \rho_i = \rho_j \text{ and } \theta_i \leq \theta_j \end{cases}$$

2) Parallel/perpendicular ordering: The order $\leq_{\Omega_4^{\mathbf{q}_0^u}}$ is achieved by considering that a quaternion is bigger than another with respect to \mathbf{q}_0^u if the modulus of the parallel part is bigger or if the length of parallel parts are equal and the modulus of the perpendicular part is smaller, i.e.,

$$\mathbf{q}_i \leq_{\Omega_4^{\mathbf{q}_0^u}} \mathbf{q}_j \Leftrightarrow \begin{cases} |\mathbf{q}_\parallel| < |\mathbf{q}_\parallel| \text{ or} \\ |\mathbf{q}_\parallel| = |\mathbf{q}_\parallel| \text{ and } |\mathbf{q}_\perp| \geq |\mathbf{q}_\perp| \end{cases}$$

However these ones are only partial orderings or pre-orderings, i.e., two distinct colour quaternions can verify the equality of the ordering. In order to have total orderings we propose to complete the proposed cascades with a lexicographical cascade of green, then red and finally blue as previously introduced for distance-based orderings [3].

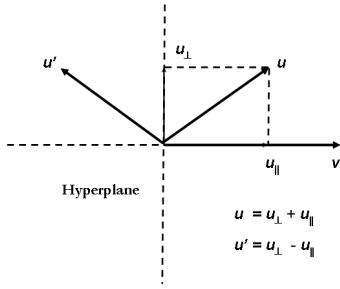


Figure 5. Decomposition of quaternion u into its projection and rejection parts according to the unitary quaternion associated to quaternion v .

Comparison with classical color total orderings

The presented lexicographical four orderings are conceptually different from the previous colour total orderings proposed in the literature. However, a comparison with previous works allows to identify some common characteristics.

In [1], an ordering based in given the priority to a linear combination of the luminance and the saturation was used to build colour levellings. At a first look, this seems similar to the ordering $\leq_{\Omega_0^{q_0}}$, using as scalar part the saturation. However, as pointed above, in this particular case the module is a combination of the saturation and a RGB energy associated to the distance from the mid-gray and not directly to an intensity of energy in the sense of the luminance.

In previous works many attention has been paid to define total orderings adapted to the hue, considered as an angular component defined in the unit circle [11]. We remark again that the angular component θ can be considered as an ordered function without the need to define an origin of angles. This last is required for defining a total ordering in the hue component.

The ordering $\leq_{\Omega_3^{q_0}}$, based on given the priority to the chromatic distance between each colour and the colour of reference, is fundamentally a distance-based ordering which corresponds to the framework studied previously in [3]. To this kind of ordering no major interest is found to consider the colour as a full quaternion. This is just the reason why this ordering has not been evaluated in the empirical part of this study. This type of ordering is very useful for colour filtering and the reader interested in more details can consult the paper [3].

Finally, orderings based on projecting the colour along a reference colour, and in particular the projection with respect to the gray axis, was studied in [9] to construct colour levellings. The projection principle is quite similar to the ordering $\leq_{\Omega_4^{q_0}}$, but note that here we are decomposing full quaternions with a scalar part.

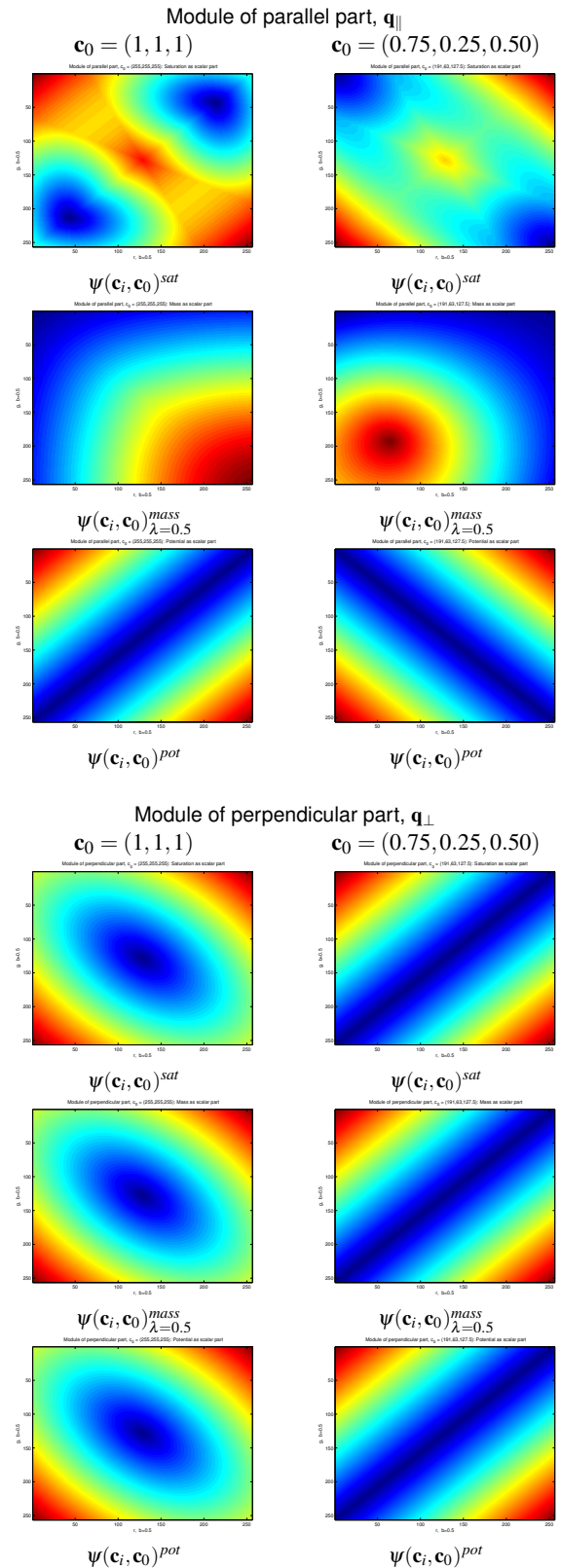


Figure 6. Variation of moduli of the parallel part $q_{\parallel i}$ and perpendicular part $q_{\perp i}$ of colour quaternions q_i , according to the different scalar parts in the plane (r, g) , $b = 0.5$, of the RGB cube. The values for two reference colours are compared.

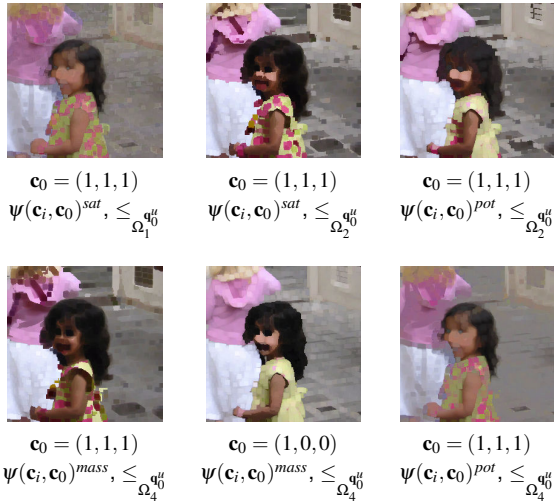


Figure 7. Comparative of colour erosions $\varepsilon_{\Omega,nB}(\mathbf{f})(x)$ (the structuring element B is a disk and the size is $n = 7$) on image “Bianca” using different quaternionic orderings and with different scalar parts.

Quaternion colour mathematical morphology

Quaternion colour erosion/dilation, opening/closing, gradient

Once a total ordering Ω has been established, the morphological colour operators are defined in the standard way.

The colour erosion of an image $\mathbf{f} \in \mathcal{F}(E, \mathcal{F}^{rgb})$ at pixel $x \in E$ by the structuring element $B \subset E$ of size n is given by

$$\varepsilon_{\Omega,nB}(\mathbf{f})(x) = \{\mathbf{f}(y) : \mathbf{f}(y) = \wedge_{\Omega}[\mathbf{f}(z)], z \in n(B_x)\}, \quad (7)$$

where \inf_{Ω} is the infimum according to the total ordering Ω . The corresponding colour dilation $\delta_{\Omega,nB}$ is obtained by replacing the \inf_{Ω} by the \sup_{Ω} , i.e.,

$$\delta_{\Omega,nB}(\mathbf{f})(x) = \{\mathbf{f}(y) : \mathbf{f}(y) = \vee_{\Omega}[\mathbf{f}(z)], z \in n(B_x)\}. \quad (8)$$

The other morphological operators, such as opening/closing, are built from the erosion and dilation. A colour opening is an erosion followed by a dilation, i.e.,

$$\gamma_{\Omega,nB}(\mathbf{f}) = \delta_{\Omega,nB}(\varepsilon_{\Omega,nB}(\mathbf{f})), \quad (9)$$

and a colour closing is a dilation followed by an erosion, i.e.,

$$\varphi_{\Omega,nB}(\mathbf{f}) = \varepsilon_{\Omega,nB}(\delta_{\Omega,nB}(\mathbf{f})). \quad (10)$$

Moreover, using a colour distance to calculate the image difference d , $d \in \mathcal{F}(E, \mathcal{F})$ (a scalar function), given by the distance point-by-point of two colour images $d(x) = \|\mathbf{f}(x) - \mathbf{g}(x)\|$. If we consider typically the Euclidean distance in RGB, we have $\|\mathbf{f}(x) - \mathbf{g}(x)\|_E = \sqrt{(f_R(x) - g_R(x))^2 + (f_G(x) - g_G(x))^2 + (f_B(x) - g_B(x))^2}$. We can easily define now the morphological colour gradient, i.e.,

$$\rho_{\Omega}(\mathbf{f})(x) = \|\delta_{\Omega,B}(\mathbf{f})(x) - \varepsilon_{\Omega,B}(\mathbf{f})(x)\|. \quad (11)$$

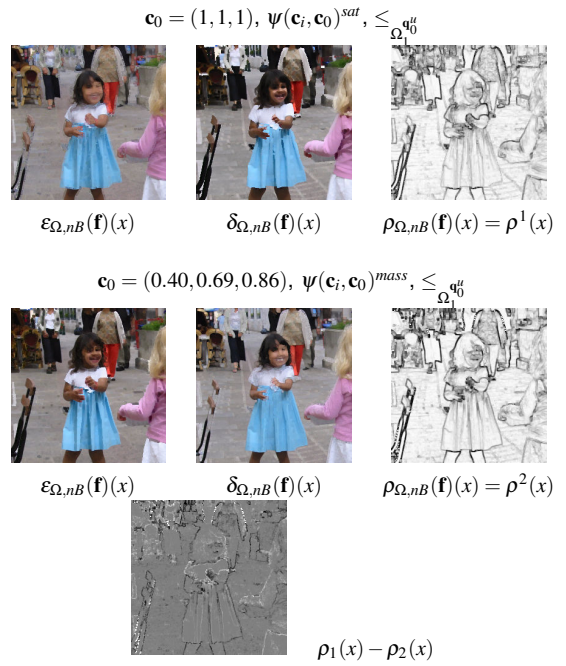


Figure 8. Comparative of two colour morphological gradients on image “Carmen”: considering the same ordering $\leq_{\Omega_1}^{q_0}$, and changing the scalar component, with the saturation and the mass (using as reference c_0 the blue colour of the skirt). First column corresponds to the isotropic erosion of size $n = 3$, second column is the associated dilation and last column is the gradient by pointwise RGB Euclidean distance between the erosion and the dilation. The last image gives the difference between both gradients (in white, pixels where $\rho_1(x)$ is bigger than $\rho_2(x)$ and in black, the dual case.)

A few examples of colour filtering

In Fig. 7 is given a comparative of erosions using different quaternionic orderings and with different scalar parts. In practice, the colour erosion shrinks the structures which have a colour close to the upper bound (“greatest colour” in the colour lattice defined by the ordering Ω) and far from the lower bound (“smallest colour”); “peaks of colour” thinner than the structuring element disappear by taking the colour of neighboring structures with a colour away from the upper bound. As well, it expands the structures which have a colour far from the upper bound. Dilation produces the dual effects, enlarging the regions having a colour close to the upper bound and contracting the others.

As we can observe in the examples, the effect of the various orderings are very different. For instance, $\leq_{\Omega_1}^{q_0}$, with saturation as scalar part, enlarges regions of chromatic colours and reduces the zones of “undefined” colours (i.e., situated in the intermediate parts of the RGB cube). The other results can be interpreted with the help of the values of quaternion parameters given in Fig. 4 and Fig. 6.

We can remark also the influence of the choice of reference colour when, for instance, the mass is taken as scalar part. In the comparative of colour gradients of Fig. 8, by choosing as reference the colour of the skirt we are sure that the associate morphological gradient to the ordering $\leq_{\Omega_1}^{q_0}$, $\psi(\mathbf{c}_i, \mathbf{c}_0)^{mass}$, will catch the contours of the image, attributing more importance to the transitions between regions close/far to the colour reference.

The last example, given in Fig. 9, deals with a comparison of colour openings. More precisely, the opening removes colour peaks that are thinner than the structuring element, having

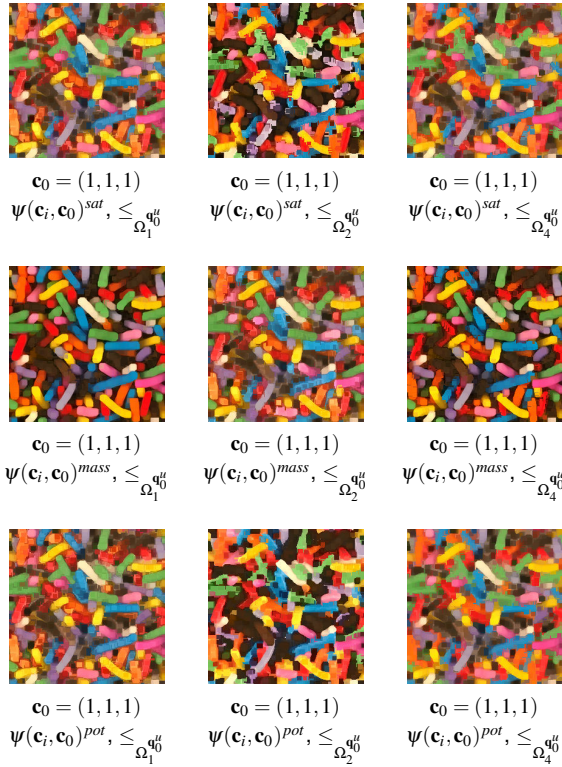


Figure 9. Comparative of colour openings $\gamma_{\Omega, nB}(\mathbf{f})(x)$ (the structuring element B is a disk and the size is $n = 7$) on image “Sweets” using different quaternionic orderings and with different scalar parts.

a colour close to the upper bound (or far from the lower bound); the closing remove colour peaks that are thinner than the structuring element, having a colour far from the upper bound (or close to the upper bound). From this example, using the same reference (white colour), it is possible to identify the orderings which yield the best visual object regularisation and the type of structures which are filtered.

Conclusions and perspectives

This paper presents two main contributions. On the one hand, we have studied different alternatives to introduce the scalar part in order to obtain full colour quaternions. On the other hand, several total lexicographic orderings for quaternions according to their different decompositions have been defined. The geometric and algebraic properties of quaternionic representations involve a rich structure to deals with ordering-based colour operations and yields a powerful framework to generalise the definition of mathematical morphology for colour images. However, deeper studies are needed to better understand the influence of the different scalar parts in the decomposition \parallel / \perp as well as to compare RGB centered colour quaternions with other kinds of RGB quaternion representations.

We have illustrated with a few examples the effects of the associated basic morphological operators to process colour images. More exhaustive empirical tests are needed to qualitatively and quantitatively compare the performances of the proposed orderings. Typically, we should evaluate the effect of quaternionic orderings to build colour connected operators (e.g., geodesic reconstruction, levellings, etc.).

In addition, we believe that other quaternion-based colour operations (colour Fourier Transform, colour convolution, etc.),

previously defined for pure colour quaternions, could be now studied for the full colour quaternions here proposed.

References

- [1] J. Angulo, J. Serra. Morphological coding of color images by vector connected filters. In *IEEE Proc. of the Seventh International Symposium on Signal Processing and Its Applications (ISSPA'2003)*, Vol. 1, p. 69–72, Paris, 2003.
- [2] J. Angulo, J. Serra. Modelling and Segmentation of Colour Images in Polar Representations. *Image and Vision Computing*, 25(4): 475–495, 2007.
- [3] J. Angulo. Morphological colour operators in totally ordered lattices based on distances. Application to image filtering, enhancement and analysis. *Computer Vision and Image Understanding*, 107(2-3): 56–73, 2007.
- [4] E. Aptoula, S. Lefèvre. A comparative study on multivariate morphology. *Pattern Recognition*, 40(11): 2914–2929, 2007.
- [5] Ph. Carré, P. Denis. Quaternionic wavelet transform for colour images. In *Wavelet Applications in Industrial Processing IV*, Vol. 6383, Boston, USA, 2006.
- [6] P. Denis, Ph. Carré, Ch. Fernandez-Maloigne. Spatial and spectral quaternionic approaches for colour images. *Computer Vision and Image Understanding*, 107(2-3):74–87, 2007.
- [7] T.A. Ell, S.J. Sangwine. Hypercomplex Wiener-Khinchine theorem with application to color image correlation. In *IEEE ICIP'00*, Vol. II, 792–795, 2000.
- [8] T.A. Ell, S.J. Sangwine. Hypercomplex Fourier transform of color images. *IEEE Transactions on Image Processing*, 16(1):22–35, 2007.
- [9] C. Gomila, F. Meyer. Levelings in Vector Spaces. In *Proc. of IEEE Conference on Image Processing*, Kobe, Japan, October 24–28, 1999.
- [10] W.R. Hamilton. *The Mathematical papers of Sir William Rowan Hamilton, Vol. III*, N. Halberstam and R.E. Ingram, Eds., Cambridge University Press, Cambridge 1967.
- [11] A. Hanbury, J. Serra. Morphological operators on the unit circle. *IEEE Transactions on Image Processing*, 10(12):1842–1850, 2001.
- [12] S.J. Sangwine, T.A. Ell. Mathematical approaches to linear vector filtering of colour images. In *CGIV'02*, 348–351, 2002.

Author Biography

Jesús Angulo received a degree in Telecommunications Engineering (1999) from Polytechnical University of Valencia, Spain, with a Master Thesis on Image and Video Processing. He obtained his PhD in Mathematical Morphology and Image Processing (2003), from the Ecole des Mines de Paris (France). He is currently a researcher in the Center of Mathematical Morphology of the Ecole des Mines de Paris. His research interests are in the areas of multivariate image processing (colour, hyper/multi-spectral, temporal series, tensor imaging) and mathematical morphology (filtering, segmentation, shape and texture analysis, stochastic approaches, geometry), and their applications to biomedicine and biotechnology.